International Journal of Cardiology 418 (2025) 132598

Contents lists available at ScienceDirect

International Journal of Cardiology

journal homepage: www.elsevier.com/locate/ijcard

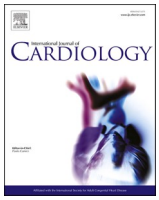

AngioPy Segmentation: An open-source, user-guided deep learning tool for coronary artery segmentation☆

Thabo Mahendiran [a,b,*], Dorina Thanou [b], Ortal Senouf [b], Yassine Jamaa [c], Stephane Fournier [a], Bernard De Bruyne [a,d], Emmanuel Abbé [b], Olivier Muller [a], Edward Andò [c]

[a] Department of Cardiology, Lausanne University Hospital, Lausanne, Switzerland
[b] Mathematical Data Science, EPFL, Lausanne, Switzerland
[c] Center for Imaging, EPFL, Lausanne, Switzerland
[d] Department of Cardiology, OLV Cardiovascular Center, Aalst, Belgium

ARTICLE INFO

Keywords:
Artificial intelligence
Deep learning
Chronic coronary syndromes
Stenosis assessment
Quantitative coronary angiography
Open source

ABSTRACT

Background: Quantitative coronary angiography (QCA) typically employs traditional edge detection algorithms that often require manual correction. This has important implications for the accuracy of downstream 3D coronary reconstructions and computed haemodynamic indices (e.g. angiography-derived fractional flow reserve). We developed *AngioPy*, a deep-learning model for coronary segmentation that employs user-defined ground-truth points to boost performance and minimise manual correction. We compared its performance without correction with an established QCA system.

Methods: Deep learning models integrating user-defined ground-truth points were developed using 2455 images from the Fractional Flow Reserve versus Angiography for Multivessel Evaluation 2 (FAME 2) study. External validation was performed on a dataset of 580 images. Vessel dimensions from 203 images with mild/moderate stenoses segmented by *AngioPy* (without correction) and an established QCA system (Medis QFR®) were compared (609 diameters).

Results: The top-performing model had an average F1 score of 0.927 (pixel accuracy 0.998, precision 0.925, sensitivity 0.930, specificity 0.999) with 99.2 % of masks exhibiting an F1 score > 0.8. Similar results were seen with external validation (F1 score 0.924, pixel accuracy 0.997, precision 0.921, sensitivity 0.929, specificity 0.999). Vessel dimensions from *AngioPy* exhibited excellent agreement with QCA ($r = 0.96$ [95 % CI 0.95–0.96], $p < 0.001$; mean difference − 0.18 mm [limits of agreement (LOA): −0.84 to 0.49]), including the minimal luminal diameter ($r = 0.93$ [95 % CI 0.91–0.95], $p < 0.001$; mean difference − 0.06 mm [LOA: −0.70 to 0.59]).

Conclusion: AngioPy, an open-source tool, performs rapid and accurate coronary segmentation without the need for manual correction. It has the potential to increase the accuracy and efficiency of QCA.

1. Introduction

Invasive X-ray coronary angiography (ICA) remains the gold standard investigation for the diagnosis of coronary artery disease (CAD). An accurate anatomical assessment of CAD is critical for subsequent clinical decision-making, such as the need for haemodynamic assessment or revascularisation [1].

Quantitative coronary angiography (QCA) provides an objective means of assessing stenosis severity [2]. Yet, despite using sophisticated edge detection algorithms that utilise pixel intensity to detect the vessel boundaries [3], current QCA systems remain prone to significant errors in vessel segmentation. ICA images are complex two-dimensional projections of three-dimensional overlapping structures (e.g. arteries, lung, bone, implanted cardiac devices), and are inherently noisy and of variable quality. As a result, vessel annotation still requires frequent and time-consuming manual correction by the user which also introduces

Abbreviations: CAD, coronary artery disease; DL, deep learning; FAME 2, Fractional Flow Reserve versus Angiography for Multivessel Evaluation 2; FFR, fractional flow reserve (FFR)-guided; FN, false negative; FP, false positive; ICA, Invasive X-ray coronary angiography; LAD, left anterior descending artery; LCX, left circumflex; LM, left main stem; OMT, optimal medical treatment; PCI, percutaneous coronary intervention; QCA, Quantitative coronary angiography; RCA, right coronary artery; TP, true positive.

☆ All authors takes responsibility for all aspects of the reliability and freedom from bias of the data presented and their discussed interpretation.

* Corresponding author at: Lausanne University Hospital, Rue du Bugnon 46, 1005 Lausanne, Switzerland.

https://doi.org/10.1016/j.ijcard.2024.132598
Received 30 July 2024; Received in revised form 18 September 2024; Accepted 23 September 2024
Available online 26 September 2024

subjectivity into an assessment that aims to be objective and reproducible [4]. This has important implications not only for the interpretation of 2D vessel contours but also the accuracy of downstream 3D coronary reconstructions and computed haemodynamic indices (e.g. angiography-derived fractional flow reserve) [5]. For this reason, amongst others, the anatomical assessment remains predominantly a visual assessment that is prone to significant inter- and intra-operator variation [6,7], as well as the overestimation of stenosis severity [8].

The abundance of ICA imaging makes coronary artery segmentation an ideal target for deep learning (DL). Numerous examples of the application of DL for coronary segmentation from ICA have been reported in the literature [9–13]. However, their potential for real-world clinical uptake is limited as they tend to perform indiscriminate segmentation of the whole coronary tree without distinguishing its branches [11] which has little clinical relevance for the interventionalist wanting to assess a particular vessel or stenosis. Furthermore, DL models for major artery segmentation only [9] exclude the possibility of analysing important side branches, which can subtend significant quantities of myocardial mass. In addition, previous DL approaches, whilst offering good overall segmentation results, are still prone to errors and issues with consistency (e.g. across different arteries).

To this end, we propose *AngioPy Segmentation* (herein referred to as *AngioPy*), an open-source, DL-driven coronary artery segmentation tool and compare its performance with an established QCA system. Critically, *AngioPy* incorporates the user's clinical expertise through the selection (via clicking) of ground-truth points along the target vessel to boost accuracy and minimise/eliminate the need for manual correction. We provide *AngioPy* as an open-source tool to facilitate further research in the field (https://gitlab.com/epfl-center-for-imaging/angiopy/angiopy-segmentation).

2. Methods

2.1. Study population

(i) Internal dataset.

For the internal dataset, ICA DICOMS were obtained from the Fractional Flow Reserve versus Angiography for Multivessel Evaluation 2 (FAME 2) trial. Details of the trial have been published previously [14]. Briefly, FAME 2 evaluated fractional flow reserve (FFR)-guided PCI plus optimal medical treatment (OMT) versus OMT alone in patients with stable coronary artery disease. For the present study, ICA examinations of patients in the control (OMT) and registry groups were included [15]. ICA images were not available for six patients and thus 561 patients were included in the final study.

(ii) External dataset.

For the external dataset, ICA DICOMS were obtained from the Future Culprit study [16]. Future Culprit is a retrospective case-control study of 83 patients hospitalised between 2008 and 2019 with an MI who had undergone ICA in the five years preceding the MI (baseline ICA). For the present study, baseline ICA images were included.

Both the FAME 2 and Future Culprit studies received full ethical approval. Both studies conformed to the ethical guidelines of the 1975 Declaration of Helsinki as reflected in a priori approval by the participant institution's human research committee.

2.2. Expert annotation

For both datasets, ground truth masks were produced by qualified interventional cardiologists who performed manual coronary artery segmentation using specialised in-house software and a customised tablet with stylus. Manual segmentation was performed for each major epicardial vessel (left anterior descending artery (LAD), left circumflex (LCx), right coronary artery (RCA)). In addition, in the internal dataset, masks for the left main stem (LM) (if clearly visible) and any major branches (proximal vessel diameter ~ 2 mm or more) were also produced.

For a given patient, and a given artery, the annotation protocol consisted of the following steps: (i) A DICOM file with the artery clearly visible with minimal foreshortening was selected; (ii) An end-diastolic frame was selected from the DICOM; (iii) Manual segmentation was performed using the customised tablet and stylus; (iv) Crucially, a set of 5–10 ground truth points (points in the true artery) along the length of the artery were then defined including the start and end of segmentation, to guide the segmentation process; (v) Steps (i) to (iv) were repeated for a second view of the same artery (ideally as close to orthogonal as possible), if available.

The final internal and external datasets consisted of 2455 and 580 labelled images, respectively.

2.3. Neural networks

Deep learning models were constructed using the U-Net architecture for semantic segmentation [17], but with replacement of the backbone of U-Net with three popular state-of-the-art architectures that have been shown to perform well with image segmentation tasks: ResNet101 [18], DenseNet121 [19], and InceptionResNet-v2 [20]. ResNet uses skip connections between consecutive layers to facilitate the training process, whilst DenseNet is a variant of ResNet that uses skip connections from each layer to every other layer (hence dense). Each block of the InceptionResNet architecture incorporates branching layers of filters of different sizes which promotes the representation of features of different resolutions. Input images of 512 × 512 pixels were normalized with 2-D min/max normalisation. Initial weights were adopted from ImageNet for transfer learning.

Critically, the input image was then modified to integrate the user's clinical expertise through the addition of the ~5 ground-truth points in separate channels in the input image. A first channel was added that stored the coordinates of the start and end points of segmentation. A further channel was added that stored the remaining ground truth points (i.e. those between the desired start and end points). Accordingly, the final input image shape used for training was 3 × 512 × 512. By incorporating ground-truth points into the input image, i.e. points that should appear in the final mask, the segmentation of areas of the image where the vessel edge was ambiguous (e.g. vessel branch, overlapping vessel) could be guided by nearby ground-truth points. This approach was hypothesised to reduce the risk of unwanted excursions away from the true vessel lumen and thus boost segmentation performance.

2.4. Experimental setup

(i) Training and testing

The models were trained in Python using the Pytorch library using two NVIDIA A100 80GB GPUs. Models were trained for a maximum of 150 epochs, using an Adam optimizer with $\beta_1 = 0.9$, $\beta_2 = 0.999$, and a mini-batch size of 10. The learning rate, which was initially set to 10^{-3}, was reduced by half up to less than 10^{-6} each time the validation loss remained saturated for 20 epochs. Data augmentation was performed with random rotation (−30° to 30°), translation shift (−20–20 % of image size in horizontal and vertical axes), and zoom (−20–20 %).

The internal dataset was divided into five folds at random and five-fold cross-validation was performed using the following proportions 3:1:1 for training, validation, and test sets, respectively.

The models trained on the internal dataset were then tested on the external dataset.

(ii) Loss function

The loss function consisted of generalized dice loss (GDL), which provides information on global segmentation quality, and focal loss (FL), which provides a pixel-wise evaluation focused on the harder-to-classify pixels [21,22]. The loss function used was:

$$\text{Loss} = \text{GDL} + \text{FL}$$

(iii) Evaluation metrics

The evaluation metrics used to assess the predictive performance of the deep learning models were: precision, recall, specificity, accuracy, and F1 score which were defined using the following equations where TP is true positive, FP is false positive, and FN is false negative:

- precision = TP/(TP + FP)
- recall = TP/(TP + FN)
- specificity = TN/(TN + FP)
- accuracy = (TP + TN)/(TP + TN + FP + FN)
- F1 = 2 × precision × recall/ (precision + recall)

2.5. Comparison with QCA

A total of 203 ICA frames from the Future Culprit study were analysed with an established commercial QCA package (Medis QFR®) to obtain vessel diameters at the site of coronary stenoses (proximal, distal, and minimal luminal diameter (MLD)). Segmentation with the QCA system was performed as per standard instructions provided by the manufacturer, with automatically detected contours corrected by the operator as required. Segmentation using *AngioPy* was then performed on the same frames by a separate operator who was aware of the vessel to be segmented but blinded to the QCA output.

In a final step, the segmentation output of the two approaches was compared. The locations of the measured vessel diameters were extracted from the QCA output and applied to a Euclidean distance transform map of the *AngioPy* segmentation mask to automatically calculate the equivalent diameter at the same location as detected by *AngioPy* [23]. A total of 609 vessel diameter measurements were compared.

2.6. Web application

In order to turn the trained DL model into a user-friendly tool, a web application was created using Python version 3.8.10 and Streamlit version 1.25.0. A demonstration of the web application along with the source code (including the final segmentation model) is available online (https://gitlab.com/epfl-center-for-imaging/angiopy/angiopy-segmentation).

2.7. Statistical analysis

Continuous values are presented as mean ± standard deviation or median and interquartile range, as appropriate. Categorical variables are presented as numbers and percentages. The association between two continuous variables was assessed using: (i) Pearson's correlation coefficient to assess for a linear correlation, and (ii) Bland-Altman analysis and the intraclass correlation coefficient (ICC) computed using a two-way mixed-effect model to assess the absolute agreement between values. Passing-Bablok regression was used in the agreement analysis comparing vessel diameters measured by QCA and *AngioPy* to assess for systematic and proportional differences. For Passing-Bablok regression analysis, no systematic bias between measurements was assumed if 95 % CI of the intercept included the value 0, whereas an absence of significant proportional bias was assumed if 95 % CI of the slope included the value 1.

Values of $p < 0.05$ were considered statistically significant. Statistical analyses were performed using Python version 3.8.10.

3. Results

3.1. Model performance with internal dataset

The baseline characteristics of the patients from the FAME 2 study have been reported previously [15], and are summarised in Supplementary Table 1. The distribution of the segmented arteries in the internal dataset is shown in **Supplementary Fig. 1**, with all major vessels being well represented. In addition, arteries were segmented from images acquired from a wide range of classically utilised incidences employed during ICA (**Supplementary Fig. 2**).

Table 1 shows the performance of the three trained DL models in the test set during five-fold cross-validation. Examples of test set inputs, ground-truth labels and DL model outputs are shown in Fig. 1. The mean F1 scores were 0.925 ± 0.0021, 0.927 ± 0.0017, and 0.927 ± 0.0012, for ResNet101, DenseNet121, and InceptionResNet-v2, respectively. F1 scores were consistently high in the test set with over 99 % of masks having an F1 score > 0.8 (ResNet101: 99.4 %, DenseNet121: 99.5 %, InceptionResNet-v2: 99.3 %).

All models performed equivalently well on the internal dataset with no statistically significant differences between models with regards to F1 score, recall, precision, accuracy or specificity. In addition, all models performed well, regardless of the target artery, although the highest F1 scores were seen with the RCA (ResNet101: 0.939 ± 0.0015, DenseNet121: 0.940 ± 0.0012, InceptionResNet-v2: 0.940 ± 0.0019) (**Supplementary Table 2**).

3.2. Model performance with external dataset

The three DL models also demonstrated excellent performance in the external dataset (Table 2). The mean F1 scores were 0.925 ± 0.0021, 0.924 ± 0.028, and 0.924 ± 0.028, for ResNet101, DenseNet121, and InceptionResNet-v2, respectively.

As seen with the internal dataset, F1 scores were consistently high with over 99 % of masks having an F1 score > 0.8 (ResNet101: 99.8 %, DenseNet121: 99.5 %, InceptionResNet-v2: 99.7 %). All models performed well on all three major epicardial arteries, with the RCA exhibiting the highest F1 scores (ResNet101: 0.935 ± 0.019, DenseNet121: 0.935 ± 0.019, InceptionResNet-v2: 0.935 ± 0.020) (**Supplementary Table 3**).

3.3. AngioPy vs QCA

Examples of artery contours produced by *AngioPy* (using the InceptionResNet-v2 encoder) and QCA (Medis QFR®) are shown in Fig. 2A. Compared with diameters measured with QCA, diameters measured with *AngioPy* (without correction) exhibited excellent correlation ($r = 0.96$, 95 % CI 0.95–0.96, $p < 0.001$) and absolute agreement (ICC = 0.96, 95 % CI 0.95–0.96, $p < 0.001$; mean difference − 0.18 mm [limits of agreement: −0.84 to 0.49]) (Fig. 2B + **C**). Passing-Bablok regression analysis found no significant systematic bias (intercept A:

Table 1
Comparison of the segmentation performance of deep learning models with the internal dataset. Mean values of metrics along with standard deviations between folds are presented.

Metric	ResNet101	DenseNet121	InceptionResNet-v2
F1	0.925 ± 0.0021	0.927 ± 0.0017	0.927 ± 0.0012
Recall	0.929 ± 0.0024	0.930 ± 0.0023	0.930 ± 0.0030
Precision	0.924 ± 0.0032	0.925 ± 0.0029	0.925 ± 0.0027
Accuracy	0.997 ± 0.0000	0.998 ± 0.0001	0.998 ± 0.0000
Specificity	0.999 ± 0.0001	0.999 ± 0.0001	0.999 ± 0.0001

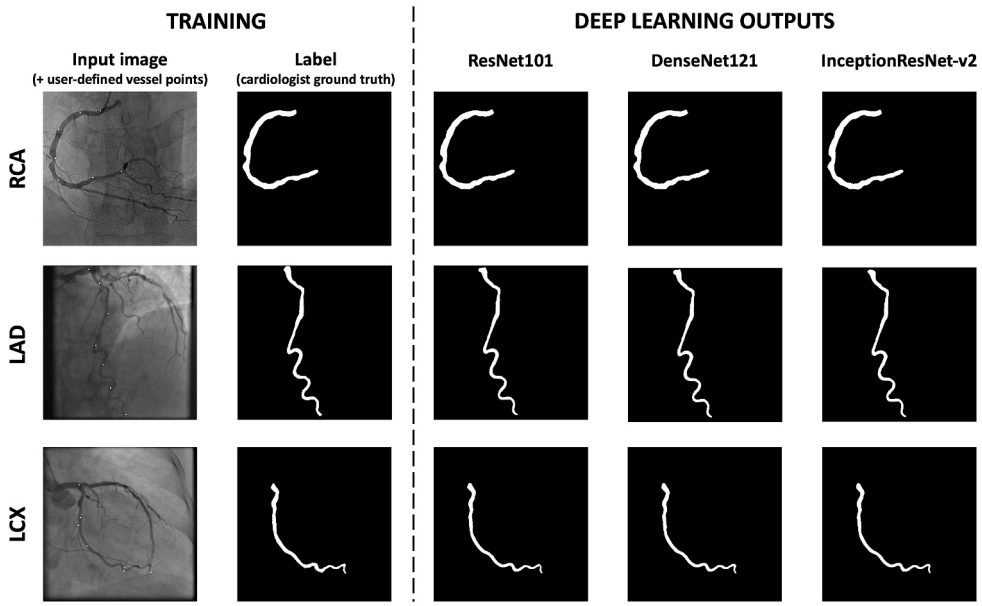

Fig. 1. Examples of major vessel segmentation by the three trained DL models. Columns from left to right: an input image from the test set (including ground truth points), the label (mask provided by cardiologist), outputs from ResNet101, DenseNet121, and InceptionResNet-v2.

Table 2
Comparison of the segmentation performance of deep learning models with the external dataset. Mean values of metrics along with standard deviations within the external dataset are presented.

Metric	ResNet101	DenseNet121	InceptionResNet-v2
F1	0.924 ± 0.029	0.924 ± 0.028	0.924 ± 0.028
Recall	0.929 ± 0.036	0.928 ± 0.036	0.929 ± 0.037
Precision	0.920 ± 0.046	0.922 ± 0.043	0.921 ± 0.044
Accuracy	0.997 ± 0.001	0.997 ± 0.001	0.997 ± 0.001
Specificity	0.999 ± 0.001	0.999 ± 0.001	0.999 ± 0.001

0.04 [−0.04–0.13]) but a weak proportional bias (slope B: 1.04 [1.02–1.07]).

MLD measurements from *AngioPy* exhibited excellent agreement with QCA ($r = 0.93$, 95 % CI 0.91–0.95; ICC = 0.93, 95 % CI 0.91–0.95, both $p < 0.001$; mean difference − 0.06 mm [limits of agreement: −0.70 to 0.59]) (Fig. 2D + **E**). Additionally, Passing-Bablok regression analysis found no significant systematic (intercept A: −0.10 [−0.28–0.08]) or proportional bias (slope B: 1.06 [1.00–1.12]).

A summary of the study findings is shown in the **Graphical Abstract**. A video example of segmentation by *AngioPy* is shown in **Supplementary Video 1**.

4. Discussion

We present *AngioPy*, an open-source, DL model for coronary artery segmentation from ICA. The principal findings of this study can be summarised as follows:

i. We demonstrate the feasibility of a user-guided, DL-driven segmentation approach that integrates user expertise via a set of rapid clicks along the artery to boost performance
ii. Models trained on images from the FAME 2 study demonstrated excellent segmentation performance that generalized well to an external dataset
iii. Segmentation masks from *AngioPy* without manual correction demonstrated excellent agreement with an established QCA system, highlighting the validity of a DL-driven segmentation approach over traditional edge detection algorithms

4.1. The limitations of QCA

Whilst a range of QCA systems are now available [24–27], current systems present practical limitations that have limited uptake into routine clinical practice. Notably, commonly employed edge detection algorithms are prone to significant errors in vessel segmentation. ICA images are complex two-dimensional projections of three-dimensional overlapping structures (e.g. arteries, lung, bone, implanted cardiac devices), and are inherently noisy and of variable quality. As a result, automatically detected vessel contours still require frequent and time-consuming manual correction by the user. Whilst there are limited data on the amount of manual correction required with current QCA systems, reported figures vary from ~10 % to ~30 % of analysed vessels [24,28]. This figure likely varies significantly depending on the QCA system being used, the quality of images, as well as the user.

Crucially, manual correction introduces subjectivity into an assessment that aims to be objective and reproducible. In fact, even in the core lab setting, QCA exhibits marked variability when the same images are analysed by different core labs [4]. This variation is concerning as it has important downstream consequences. Firstly, it affects the interpretation of lesion severity directly from the 2D vessel contours. Secondly, it affects the accuracy of the 3D geometries generated by QCA as these are highly dependent on the quality of the original arterial segmentation. Inaccurate segmentation produces inaccurate 3D geometries, and this also has implications for downstream haemodynamic simulations (e.g. virtual computation of FFR). Westra et al. reported significant intra- and inter-operator variability in the calculation of quantitative flow ratio (QFR) from the same ICA images, with marked variability in the use of manual correction [5]. This, at least in part, may help to explain the imperfect agreement between angiography-derived FFR and pressure wire-based FFR [29].

4.2. The potential of DL-driven approaches

Examples of the application of DL for coronary segmentation from ICA have been reported in the literature [9–12]. However, their potential for real-world clinical uptake is limited as they tend to perform indiscriminate segmentation of the whole coronary tree [11], or just the major coronary arteries without important branches [9]. For example, Yang et al. trained a DL model for major coronary vessel segmentation (i.

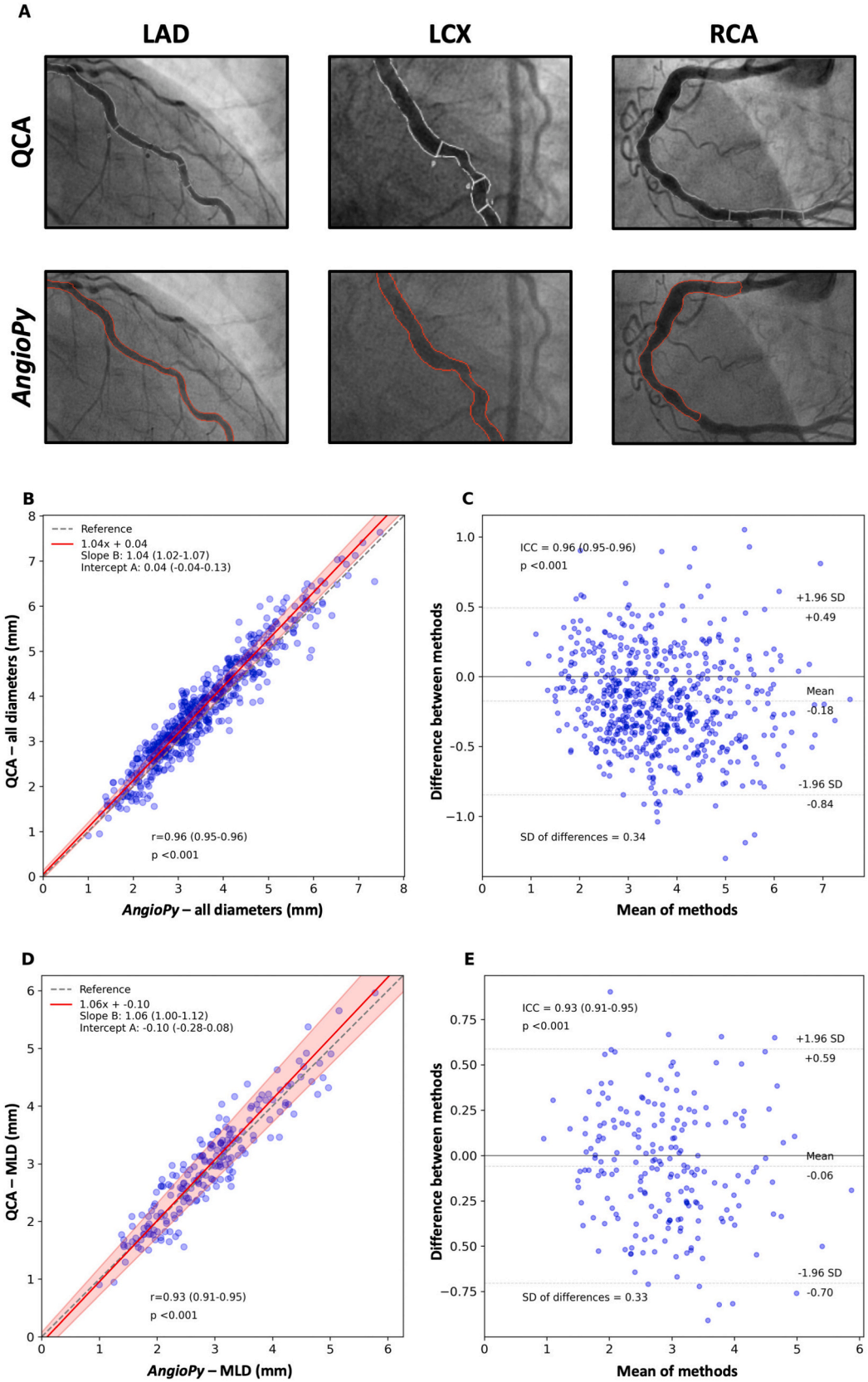

Fig. 2. *AngioPy* vs QCA: (**A**) examples of artery contours produced by an established QCA system and *AngioPy*; agreement between *AngioPy* and QCA for all vessel diameters (**B** + **C**), and for lesion MLD (**D** + **E**).

e. LAD, LCX, RCA) with an average F1 score of 0.917 and 93.7 % of masks exhibiting an F1 score > 0.8 [9]. Iyer et al. developed AngioNet, a DL model that segmented the whole coronary tree from an ICA frame with an average F1 score of 0.864 [11]. Most recently, Liu et al. presented AI-QCA, a DL model that segments major epicardial vessels as well as their branches [13]. Whilst this represented progress in the field, the reported F1 score of 0.879 was not an improvement on previously reported data. Furthermore, agreement with QCA measurements was moderate (e.g. Pearson's *r* for MLD = 0.765).

AngioPy presents several advantages over previously reported work. Firstly, it directly integrates the user's clinical expertise through the rapid selection of a handful of ground truth points along the vessel to guide the segmentation process. This permits the segmentation of any coronary vessel including side branches, with the interface providing the user with complete control over the choice of vessel, as well as the start and endpoint point of segmentation. This approach resulted in excellent segmentation performance with an average F1 score of 0.927. Furthermore, this approach resulted in consistently high-level segmentation with over 99 % of masks exhibiting an F1 score > 0.8. This consistency was also exemplified by the consistent segmentation performance across artery types (mean F1 scores: LAD 0.922, RCA 0.940, LCX 0.920, LM 0.930) which was markedly better than the inter-arterial variation previously reported [9,13].

Our study also demonstrated the excellent generalisability of *AngioPy* to an external dataset. In addition to the integration of user-defined ground truth points, this generalisability is likely also thanks to the diversity of the training dataset. The ICA images from FAME 2 come from 28 different centres (in Europe, the U.S., and Canada) representing a range of different coronary angiography machines, variable image quality, as well as variability in image acquisition practices such as the incidences used (**Supplementary Fig. 2**).

Finally, vessel diameters measured from uncorrected *AngioPy* segmentation masks demonstrated excellent agreement with QCA, highlighting that a DL-driven approach can produce similar results, whilst avoiding manual correction and its associated time cost and risk of subjectivity. Of note, the weak proportional bias (1.04) can be considered clinically insignificant given its small size.

Ultimately, these results suggest the potential for faster and more reproducible segmentation with *AngioPy* that opens the door to the use of QCA "live" during ICA in a way that could influence clinical decision-making. This is in contrast to current QCA systems which are typically used "offline" after the procedure, with the patient no longer on the cardiac catheterisation table. Further work is now needed to demonstrate the feasibility and efficacy of using *AngioPy* "online" in a real-world catheterisation laboratory setting.

4.3. Open-source software

Currently, available QCA systems are proprietary, closed source and purchased at a significant cost. This creates significant barriers to their use in both clinical and research contexts. As such we release *AngioPy* as an open-source tool to promote innovation and advancements in the field (https://gitlab.com/epfl-center-for-imaging/angiopy/angiopy-segmentation).

4.4. Limitations

First, *AngioPy* still requires the user to select an ICA frame for segmentation. Whilst the identification of an optimal end-diastolic frame for segmentation could easily be automated with a DL-based approach, this was not a goal of the present study. Second, whilst *AngioPy* permits the segmentation of any coronary artery including major branches, the accuracy of bifurcation segmentation was not evaluated. Previous studies have shown single-vessel QCA software to be inaccurate in this setting due to the specific anatomical characteristics of bifurcations [30]. Further work will aim to assess the validity of *AngioPy* in the assessment of bifurcations and bifurcation lesions specifically. Third, previous deep learning models developed for ICA have either not been released as open-source, or have been released without pre-trained model weights. As a result, a direct comparison of *AngioPy* with these previous methods was not possible. This limitation further highlights the importance of open-source code and vindicates our decision to release the source code of *AngioPy* for the wider community. Finally, we did not perform a formal comparison of the time required to perform segmentation with *AngioPy* and QCA. However, segmentation takes just seconds with *AngioPy*, and given that manual correction is not required, we believe that the use of *AngioPy* results in ultimately faster and more consistent segmentation.

5. Conclusion

AngioPy performs rapid and accurate coronary segmentation of any vessel without the need for manual correction and compares favourably with an established QCA system. Available as an open-source tool, *AngioPy* has the potential to increase the efficiency and reliability of QCA.

Funding

TM is supported by a research grant from the Swiss National Science Foundation (SNSF).

CRediT authorship contribution statement

Thabo Mahendiran: Writing – review & editing, Writing – original draft, Software, Methodology, Investigation, Formal analysis, Data curation, Conceptualization. **Dorina Thanou:** Writing – review & editing, Methodology. **Ortal Senouf:** Writing – review & editing, Methodology. **Yassine Jamaa:** Writing – review & editing, Methodology, Investigation, Formal analysis. **Stephane Fournier:** Writing – review & editing, Data curation. **Bernard De Bruyne:** Writing – review & editing, Supervision, Data curation. **Emmanuel Abbé:** Writing – review & editing, Supervision, Methodology. **Olivier Muller:** Writing – review & editing, Supervision. **Edward Andò:** Writing – review & editing, Supervision, Software, Methodology, Investigation, Formal analysis, Conceptualization.

Declaration of competing interest

BDB reports receiving consultancy fees from Boston Scientific and Abbott Vascular, research grants from Coroventis Research, Pie Medical Imaging, CathWorks, Boston Scientific, Siemens, HeartFlow Inc., and Abbott Vascular, and owning equity in Siemens, GE, Philips, HeartFlow Inc., Edwards Life Sciences, Bayer, Sanofi, Celyad.

All the other authors have nothing to disclose.

Supplementary data to this article can be found online at https://doi.org/10.1016/j.ijcard.2024.132598.

Data availability

The imaging data underlying this article will be shared on reasonable request to the corresponding author. The code for *AngioPy Segmentation* including the trained segmentation model is available via the following link:https://gitlab.com/epfl-center-for-imaging/angiopy/angiopy-segmentation.

References

[1] J. Knuuti, W. Wijns, A. Saraste, D. Capodanno, E. Barbato, C. Funck-Brentano, et al., 2019 ESC guidelines for the diagnosis and management of chronic coronary syndromes, Eur. Heart J. 41 (3) (2020) 407–477.

[2] D. Keane, J. Haase, C.J. Slager, E. Montauban van Swijndregt, K.G. Lehmann, Y. Ozaki, et al., Comparative validation of quantitative coronary angiography

systems. Results and implications from a multicenter study using a standardized approach, Circulation 91 (8) (1995) 2174–2183.
[3] F. Alfonso, Videodensitometric vs edge-detection quantitative angiography. Insights from intravascular ultrasound imaging, Eur. Heart J. 21 (8) (2000) 604–607.
[4] M.J. Grundeken, Y. Ishibashi, P. Généreux, L. LaSalle, J. Iqbal, J.J. Wykrzykowska, et al., Inter–core lab variability in analyzing quantitative coronary angiography for bifurcation lesions: a post-hoc analysis of a randomized trial, J. Am. Coll. Cardiol. Intv. 8 (2) (2015) 305–314.
[5] J. Westra, M. Sejr-Hansen, L. Koltowski, H. Mejía-Rentería, S. Tu, J. Kochman, et al., Reproducibility of quantitative flow ratio: the QREP study, EuroIntervention 17 (15) (2022) 1252–1259.
[6] Herrman JPR, Azar A, Umans VA, Boersma E, Serruys PW, others. Inter-and intra-observer variability in the qualitative categorization of coronary angiograms Int. J. Card. Imaging 1996;12(1):21–30.
[7] R. Shah, E. Yow, W.S. Jones, L.P. Kohl III, A.S. Kosinski, U. Hoffmann, et al., Comparison of visual assessment of coronary stenosis with independent quantitative coronary angiography: findings from the prospective multicenter imaging study for evaluation of chest pain (PROMISE) trial, Am. Heart J. 184 (2017) 1–9.
[8] B.K. Nallamothu, J.A. Spertus, A.J. Lansky, D.J. Cohen, P.G. Jones, F. Kureshi, et al., Comparison of clinical interpretation with visual assessment and quantitative coronary angiography in patients undergoing percutaneous coronary intervention in contemporary practice, Circulation 127 (17) (2013) 1793–1800.
[9] S. Yang, J. Kweon, J.H. Roh, J.H. Lee, H. Kang, L.J. Park, et al., Deep learning segmentation of major vessels in X-ray coronary angiography, Sci. Rep. 9 (1) (2019). Available from: http://www.nature.com/articles/s41598-019-53254-7.
[10] T.J. Jun, J. Kweon, Y.H. Kim, D. Kim, T-net: nested encoder–decoder architecture for the main vessel segmentation in coronary angiography, Neural Netw. 128 (2020) 216–233.
[11] K. Iyer, C.P. Najarian, A.A. Fattah, C.J. Arthurs, S.M.R. Soroushmehr, V. Subban, et al., AngioNet: a convolutional neural network for vessel segmentation in X-ray angiography, Sci. Rep. 11 (1) (2021) 18066.
[12] S. Yang, J. Kweon, Y.H. Kim, Major Vessel Segmentation on X-ray Coronary Angiography Using Deep Networks With a Novel Penalty Loss Function, 13 [cited 2023 Apr 18]. Available from, https://openreview.net/forum?id=H1lTh8unKN, 2022.
[13] X. Liu, X. Wang, D. Chen, H. Zhang, Automatic quantitative coronary analysis based on deep learning, Appl. Sci. 13 (5) (2023) 2975.
[14] P. Xaplanteris, S. Fournier, N.H.J. Pijls, W.F. Fearon, E. Barbato, P.A.L. Tonino, et al., Five-year outcomes with PCI guided by fractional flow reserve, N. Engl. J. Med. 379 (3) (2018) 250–259.
[15] G. Ciccarelli, E. Barbato, G.G. Toth, B. Gahl, P. Xaplanteris, S. Fournier, et al., Angiography versus hemodynamics to predict the natural history of coronary Stenoses: fractional flow reserve versus angiography in multivessel evaluation 2 substudy, Circulation 137 (14) (2018) 1475–1485.
[16] M. Pagnoni, D. Meier, A. Candreva, L. Maillard, J. Adjedj, C. Collet, et al., Future culprit detection based on angiography-derived FFR, Catheter. Cardiovasc. Interv. 98 (3) (2021) E388–E394.
[17] O. Ronneberger, P. Fischer, T. Brox, U-NET: Convolutional networks for biomedical image segmentation, in: International Conference on Medical Image Computing and Computer-Assisted Intervention, Springer, 2015, pp. 234–241.
[18] K. He, X. Zhang, S. Ren, J. Sun, Deep Residual Learning for Image Recognition, 2016, p. 770.
[19] G. Huang, Z. Liu, L. Van Der Maaten, K.Q. Weinberger, Densely connected convolutional networks, in: 2017 IEEE Conference on Computer Vision and Pattern Recognition (CVPR) [Internet], 2017, pp. 2261–2269 [cited 2024 Apr 9]. Available from: https://ieeexplore.ieee.org/document/8099726.
[20] C. Szegedy, W. Liu, Y. Jia, P. Sermanet, S. Reed, D. Anguelov, et al., Going deeper with convolutions, in: 2015 IEEE Conference on Computer Vision and Pattern Recognition (CVPR) [Internet], 2015, pp. 1–9 [cited 2024 Apr 9]. Available from: https://ieeexplore.ieee.org/document/7298594.
[21] J.L. Silva, M.N. Menezes, T. Rodrigues, B. Silva, F.J. Pinto, A.L. Oliveira, Encoder-Decoder Architectures for Clinically Relevant Coronary Artery Segmentation [Internet] [cited 2023 Apr 18]. Available from: http://arxiv.org/abs/2106.11447, 2021.
[22] T.Y. Lin, P. Goyal, R. Girshick, K. He, P. Dollár, Focal loss for dense object detection, in: 2017 IEEE International Conference on Computer Vision (ICCV) [Internet], 2017, pp. 2999–3007 [cited 2024 Apr 9] Available from: https://ieeexplore.ieee.org/document/8237586.
[23] P. Virtanen, R. Gommers, T.E. Oliphant, M. Haberland, T. Reddy, D. Cournapeau, et al., SciPy 1.0: fundamental algorithms for scientific computing in Python, Nat. Methods 17 (3) (2020) 261–272.
[24] K. Masdjedi, N. Tanaka, E. Van Belle, S. Porouchani, A. Linke, F.J. Woitek, et al., Vessel fractional flow reserve (vFFR) for the assessment of stenosis severity: the FAST II study, EuroIntervention 17 (18) (2022) 1498–1505.
[25] G. Witberg, T. Bental, A. Levi, Y. Talmor-Barkan, A. Rotholz, T. Tanigaki, et al., Clinical outcomes of FFRangio-guided treatment for coronary artery disease, J. Am. Coll. Cardiol. Intv. 15 (4) (2022) 468–470.
[26] J. Jiang, L. Tang, C. Du, X. Leng, J. He, Y. Hu, et al., Diagnostic performance of AccuFFRangio in the functional assessment of coronary stenosis compared with pressure wire-derived fractional flow reserve, Quant. Imaging Med. Surg. 12 (2) (2022) 94958.
[27] B.K. Andersen, M. Sejr-Hansen, J. Westra, G. Campo, A. Efterkhari, S. Tu, et al., Quantitative flow ratio versus fractional flow reserve for guiding percutaneous coronary intervention: design and rationale of the randomised FAVOR III Europe Japan trial, EuroIntervention 18 (16) (2023) e1358–e1364.
[28] A. Milzi, R. Dettori, N. Marx, S. Reith, M. Burgmaier, Quantitative flow ratio (QFR) identifies functional relevance of non-culprit lesions in coronary angiographies of patients with acute myocardial infarction, Clin. Res. Cardiol. 110 (10) (2021) 1659–1667.
[29] R. Kornowski, I. Lavi, M. Pellicano, P. Xaplanteris, H. Vaknin-Assa, A. Assali, et al., Fractional flow reserve derived from routine coronary angiograms, J. Am. Coll. Cardiol. 68 (20) (2016) 2235–2237.
[30] M.J. Grundeken, Y. Ishibashi, S. Ramcharitar, J.C. Tuinenburg, J.H.C. Reiber, S. Tu, et al., The Need for Dedicated Bifurcation Quantitative Coronary Angiography (QCA) Software Algorithms to Evaluate Bifurcation Lesions [Internet], Available from: https://eurointervention.pcronline.com/article/the-need-for-dedicated-bifurcation-quantitative-coronary-angiography-qca-software-algorithms-to-evaluate-bifurcation-lesions, 2024.